

# Transformation of $\beta$ -SiC from Charcoal, Coal, and Petroleum Coke to $\alpha$ -SiC at Higher Temperatures



SETHULAKSHMY JAYAKUMARI and MERETE TANGSTAD

SiC is one of the main intermediate compounds formed during the industrial production of silicon (Si). In the Si process, SiC is produced when carbon added to the raw materials reacts with the silicon monoxide gas (SiO(g)) formed in the furnace. Carbon materials used are either biomass-based (charcoal and wood chips) or based on fossil sources (coal, coke, petroleum coke). The most common forms of SiC prevailing at atmospheric pressure are the polytypes of  $\alpha$ -SiC and  $\beta$ -SiC.  $\beta$ -SiC is formed at low temperatures and transforms to  $\alpha$ -SiC at higher temperatures ( $> 2000$  °C). In this study,  $\beta$ -SiC with elemental Si of varying amounts, formed from industrial carbon materials (charcoal, coal, and petroleum coke), were utilized to study the transformation of  $\beta$ -SiC to  $\alpha$ -SiC. A graphite tube furnace efficient for high-temperature experiments was utilized for the heat treatment of  $\beta$ -SiC particles at temperatures ranging from 2100 °C to 2450 °C. The transformation to  $\alpha$ -SiC was greatly influenced by the original carbon source. Charcoal-converted  $\beta$ -SiC particles easily transformed to  $\alpha$ -SiC at 2100 °C, compared with  $\beta$ -SiC produced from coal and petroleum coke. Moreover, the amount of elemental Si in SiC particles enhanced the transformation to  $\alpha$ -SiC at 2100 °C.

<https://doi.org/10.1007/s11663-020-01970-1>  
© The Author(s) 2020

## I. INTRODUCTION

SILICON carbide (SiC) is a non-oxidic ceramic material. Its excellent electronic properties make SiC a highly promising material for many industrial applications.<sup>[1,2]</sup> SiC has higher hardness and mechanical strength at higher temperatures, and excellent thermal conductivity. It also has a low coefficient of thermal expansion, high melting point, high resistance to corrosion and oxidation, and a wide bandgap. Various methods are used for manufacturing SiC, such as the Acheson's process, physical vapor deposition (PVD) and chemical vapor deposition (CVD).<sup>[3]</sup> SiC is also a significant compound in the industrial silicon (Si) production process.<sup>[4]</sup> In the Si furnace, a part of the carbon (C) sources converts to SiC as a result of its interaction with the silicon monoxide gas (SiO(g)) produced in the furnace.<sup>[5,6]</sup> The most commonly used carbonaceous materials in the industrial production of Si are charcoal, coal, and petroleum coke.

SiC is the only compound that combines Si and carbon atoms in a tetrahedral coordination.<sup>[7,8]</sup> SiC exists in different crystallographic forms, called polytypes. Polytypes differ from each other in their atomic layer sequencing, which influences the crystallographic growth direction.<sup>[9-13]</sup> All polytypes of SiC have the same composition, and the Si and carbon atoms are covalently bonded. Despite this, each SiC polytype has its own unique set of electronic properties. The polytypes in SiC are categorized into two main groups,  $\beta$ -SiC and  $\alpha$ -SiC, and are identified by a number and a letter. The number represents the total number of tetrahedron layers in the stacking sequence, whereas the letter identifies the shape of the unit cell. SiC polytypes with cubic symmetry called 3C-SiC (here C denotes cubic) belong to the  $\beta$ -SiC group and the remaining polytypes with hexagonal (H) and rhombohedral (R) symmetries are collectively referred to as  $\alpha$ -SiC. The most commonly occurring  $\alpha$ -SiC polytypes in Si production are 4H, 6H, and 15R.<sup>[10,12]</sup> The number of polytypes present in SiC determines its conductivity properties. The thermal conductivity for 3C, 4H, and 6H-SiC ranges between 3 to 5 W cm<sup>-1</sup> K<sup>-1</sup>.<sup>[1,14,15]</sup>

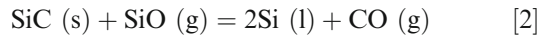
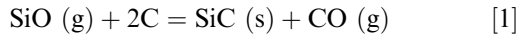
In the Si production process, the SiO reactivity is dependent on the structure, property, and type of carbon materials, and has already been studied extensively.<sup>[5,6,15]</sup> Based on the temperature distribution and chemical reactions that take place during the Si process, the interior of the furnace is divided into two: low and

---

SETHULAKSHMY JAYAKUMARI and MERETE TANGSTAD are with the Department of Materials Science and Engineering, Norwegian University of Science and Technology, Alfred Getz vei, 2B, 7034, Trondheim, Norway. Contact e-mail: sethulakshmy.jayakumari@ntnu.no.

Manuscript submitted February 16, 2020.  
Article published online October 7, 2020.

high-temperature zones, which are designated as the outer and inner reactions zones, respectively. In the outer reaction zone of the Si furnace, where the temperature ranges between 700 °C and 1800 °C, the carbon sources convert to SiC and carbon monoxide (CO) as a result of its interaction with SiO(g). The SiC formed in the outer zone will descend to the lower part of the furnace, called the inner zone, where the temperature ranges from 1800 °C to 2000 °C or more, and reacts with SiO to form Si. Both these reactions occur as follows:



A significant issue in the industrial Si process is the accumulation of SiC that has not been completely consumed at the inner zone of the furnace. Accumulation of SiC have been observed at the furnace hearth during excavations of industrial furnaces such as the 40 MW Si and 17 MW FeSi furnaces.<sup>[16–18]</sup> The structure of SiC accumulated in the crust was different compared with the structure of the carbon-converted SiC. The initially formed carbon-converted SiC had the same structure as that of the original carbon material, which was of the cubic polytype  $\beta$ -SiC (3C).<sup>[18,19]</sup> However, the SiC crust in the Si furnace was black in color, named as black-SiC, and occupied a larger volume, filling the inner parts of the entire furnace from the bottom to the top. It was assumed that the SiC crust might have formed from the transformed carbon particles. Analyses have shown that more than 90 pct of the SiC excavated from industrial Si furnace crusts consisted of  $\alpha$ -SiC.<sup>[16]</sup> Tangstad *et al.*<sup>[16]</sup> observed large gas channels in the SiC crust with precipitates of SiC in the shape of dendrites formed in these gas channels. They proposed that the accumulated carbon or SiC exposed to temperatures higher than 2000 °C formed gaseous compounds containing carbon or Si, and during cooling, at around 2000 °C, these gaseous products precipitated as  $\alpha$ -SiC.

Temperature plays an important role in transforming  $\beta$ -SiC to  $\alpha$ -SiC. The stability diagram for the occurrence of SiC polytypes as a function of temperature from Knippenberg<sup>[20]</sup>, reprinted from Jepps and Page<sup>[10]</sup>, is shown in Figure 1(a). Various studies have shown that the SiC peritectic temperature varies,<sup>[7,8]</sup> whereas the equilibrium Si-C phase diagram reproduced using FactSage software shows that SiC decomposes peritectically resulting in a Si rich liquid in equilibrium with graphite at temperatures near 2800 °C, as shown in Figure 1(b).

Yoo and Matsunami<sup>[21]</sup> investigated the thermal stability of 3C-SiC at temperatures ranging from 1800 °C to 2400 °C in an argon (Ar) atmosphere. A solid-state phase transformation from 3C to 6H, caused by the displacement of atoms *via* thermal diffusion, was observed at temperatures above 2150 °C. Lindstad<sup>[3]</sup> has shown that during the recrystallization of SiC in an Acheson furnace, nucleation of  $\beta$ -SiC grains from the gas phase initially occurred in accordance with Reaction [1], and after retaining for a longer duration at higher

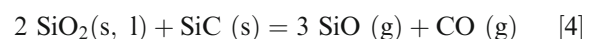
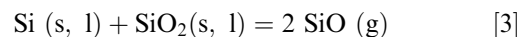
temperatures, the  $\beta$ -SiC grains grew as  $\alpha$ -SiC. Lindstad<sup>[3]</sup> also observed the quantity of  $\alpha$ -SiC decreased at temperatures above 2570 °C, and this temperature was considered as the decomposition temperature of SiC. The study inferred that the formation of gas supersaturated with Si(g), Si<sub>2</sub>(g), Si<sub>2</sub>C(g), and SiC<sub>2</sub>(g) could have diffused toward the low-temperature region and precipitated as  $\beta$ -SiC.<sup>[3]</sup>

Jayakumari and Tangstad<sup>[22,23]</sup> studied SiC formation from various carbon sources and found that the formation of SiC polytypes follows the stability diagram shown in Figure 2(a). In these studies, the SiC produced from charcoal, coal, and petroleum coke at temperatures ranging from 1750 °C to 1900 °C was confirmed as  $\beta$ -SiC and  $\alpha$ -SiC was not found in any of the samples they analyzed. Ringdalen<sup>[19]</sup> has shown that  $\beta$ -SiC from coal did not transform to  $\alpha$ -SiC at temperatures lower than 2200 °C. However, when the same  $\beta$ -SiC sample was heated at 2350 °C for 60 minutes, 66.7 wt pct of it transformed to  $\alpha$ -SiC. These studies suggest that the formation of  $\alpha$ -SiC requires temperatures higher than 2000 °C.

Though the properties of commercial SiC are well documented, the formation processes as well as properties of the various polytypes of SiC formed during the industrial production of Si are not investigated to the same extent. Knowledge about the characteristics of SiC produced from different carbon materials and the changes they undergo at high temperatures might lead to advances both in the field of electronic applications and the Si industry. To this purpose, we investigated the transformation of  $\beta$ -SiC to  $\alpha$ -SiC, based on the original type of carbon materials. We examined the influences of temperature, properties of the original carbon materials, and the presence of elemental Si in the  $\beta$ -SiC, on the extent of its transformation to  $\alpha$ -SiC. The experimental procedure and the conditions set for the transformation of  $\alpha$ -SiC are described in Section II followed by a description of the experimental results in Section III. The obtained results are explained in Section IV and finally, conclusions derived from the present study are presented in Section V.

## II. EXPERIMENTAL PROCEDURE

To study the properties of SiC at high temperatures, we produced  $\beta$ -SiC in an induction furnace in the laboratory. Charcoal, coal, and petroleum coke were used as the raw materials to produce  $\beta$ -SiC from the interaction between carbon and SiO(g) according to Reaction [1]. A mixture of (SiO<sub>2</sub> + Si) or (SiO<sub>2</sub> + SiC) was utilized to generate SiO(g) according to



Two types of SiC raw materials, *i.e.*,  $\beta$ -SiC without Si and  $\beta$ -SiC containing varying amounts of Si, were used for their further transformation to  $\alpha$ -SiC. The amount of Si in  $\beta$ -SiC was estimated quantitatively using an

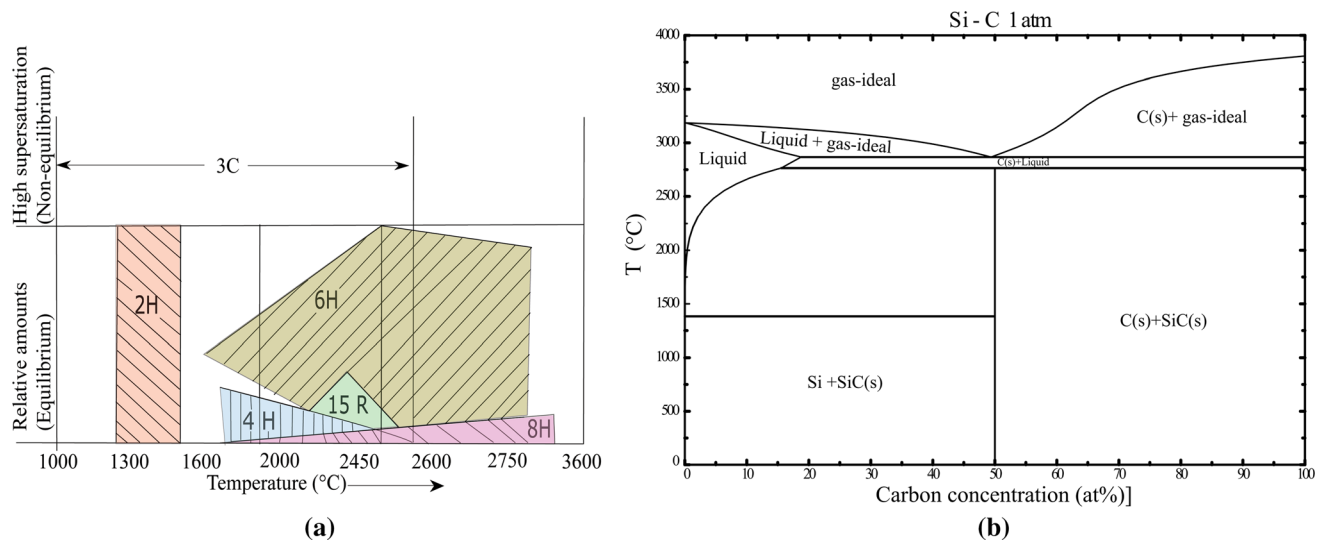


Fig. 1—(a) Stability diagram for the occurrence of SiC polytypes as function of temperature, reprinted with permission from Jepps and Page<sup>[10]</sup> and (b) equilibrium phase diagram of Si-C system.

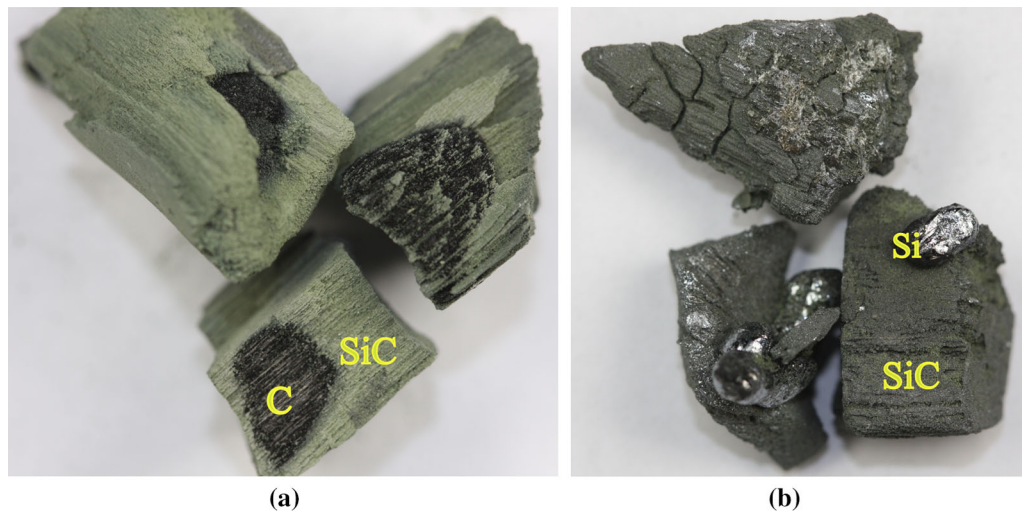


Fig. 2—Samples of  $\beta$ -SiC produced in the induction furnace. (a) Charcoal is partially converted to  $\beta$ -SiC and has unreacted carbon (C) in it. (b)  $\beta$ -SiC particles with elemental Si in it.

X-ray fluorescence (XRF) instrument. Figure 2 shows samples of  $\beta$ -SiC collected from the induction furnace; one had partially converted to SiC with some unreacted carbon left in it, and the other is SiC with varying amounts of elemental Si in it.

A graphite tube furnace consisting of a graphite chamber was used to heat the  $\beta$ -SiC samples and investigate the conversion to  $\alpha$ -SiC. The furnace was equipped with a pyrometer to constantly measure the temperatures during the experiments. The experimental setup for the heat treatment of  $\beta$ -SiC particles in the graphite chamber is illustrated in Figure 3. The graphite chamber was 250 mm tall and 150 mm in diameter and consisted of two parts; a reaction chamber and a condensation chamber. A small graphite crucible with an outer diameter of 40 mm and a height of 65 mm was placed inside the reaction chamber to heat the  $\beta$ -SiC

particles of sizes ranging between 5 and 6 mm. The whole process was done in an atmosphere of a mixture of inert gas (Ar or helium (He)) and CO, which was introduced through the gas lance mounted inside the graphite chamber. The CO gas was used to simulate the atmosphere inside an industrial Si furnace. The condensation chamber was filled with coal particles of 2 to 4 mm in size to capture the volatile matter and they also kept the gas lance fixed in position. A temperature range of 2100 °C to 2450 °C was chosen for the heat-treating experiments.

Prior to heating, the furnace chamber was purged with Ar gas flowing at rate of 0.5 L/min for 20 minutes, followed by evacuation to a residual pressure around 0.240 mbar. The graphite cylinder was then filled with Ar at 1 atm to remove the moisture and air components adsorbed on the graphite parts of the furnace. As soon



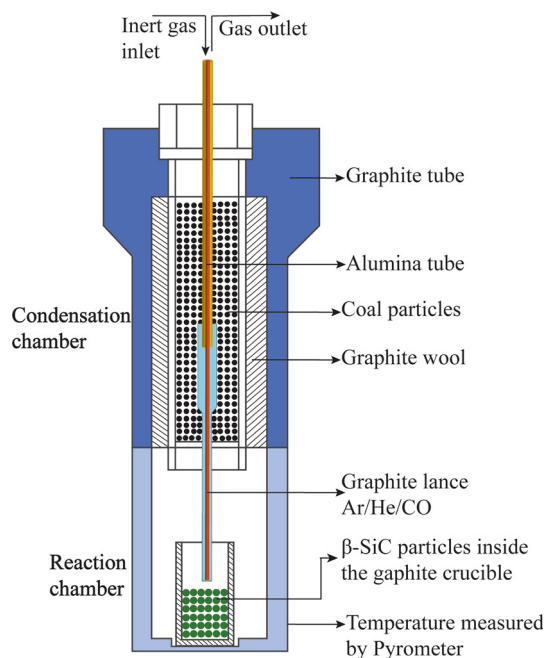


Fig. 3—Experimental setup for heat treatment of  $\beta$ -SiC particles in the graphite chamber.

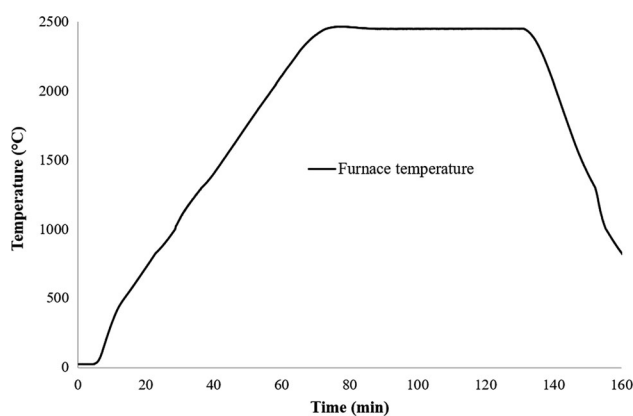


Fig. 4—Evolution of temperature inside the graphite tube furnace during the conversion of  $\beta$ -SiC to  $\alpha$ -SiC.

as the furnace started heating, a mixture of 0.5 L/min CO and 0.3 L/min Ar was injected simultaneously into the reaction chamber where the small graphite crucible containing  $\beta$ -SiC particles was placed. Figure 4 shows an example of evolution of temperature inside the furnace during the experiment. It shows the temperature profile of the experiment conducted at 2450 °C with charcoal-derived  $\beta$ -SiC. The furnace was heated to reach the target temperature at the rate of 10 °C/min. Once the temperature reached the target value, it was held for 1 hours (Figure 4). While heating the  $\beta$ -SiC particles, the inert gas was switched from Ar to He at temperatures higher than 1800 °C, to prevent ionization of Ar at higher temperatures and for safe operation of the furnace. Earlier studies have shown that a difference of ~ 15 °C exists between the temperatures measured by the pyrometer kept outside the reaction chamber and

the actual temperature measured at the bottom of the graphite crucible.<sup>[24]</sup> The initial materials used for the different experiments conducted in this study along with the conditions set for each of the experiments are detailed in Table I.

The  $\alpha$ -SiC obtained after the experiments were further analyzed to study the formation mechanisms and governing factors of the transformation procedure. To investigate the SiC phases formed after the heat treatments, the samples were analyzed using the X-ray diffraction (XRD) technique and under a scanning electron microscope (SEM). For the XRD analysis, a portion of each sample was crushed to powder in a grinding mill, using a wolfram carbide disk, and was loaded into a back-loading sample holder. The X-ray diffractograms from each sample were collected using a Bruker D8 Focus X-ray diffractometer, running in Bragg Brentano collection mode with Cu-K $\alpha$  radiation. SiC polytypes in each of the samples were quantitatively analyzed from the XRD data using Bruker Topas v5 software, a Rietveld whole pattern fitting technique. The most commonly occurring polytypes 3C, 4H, 6H, and 15R were chosen for the fitting analysis.<sup>[9]</sup> The morphology of the samples was investigated by a field-emission SEM (FESEM, Zeiss Ultra 55) with energy-dispersive X-ray spectrometers (EDX). The back-scattered electron imaging (BSE) using an electron probe micro-analyzer (EPMA; JEOL JXA-8500) was also performed for the qualitative elemental mapping of the samples.

### III. RESULTS

The surface morphologies of SiC particles before and after the heat treatment were examined under the SEM. Figure 5 shows SEM morphologies and EPMA images of  $\beta$ -SiC particles formed on the surfaces of charcoal, coal, and petroleum coke, which were used for the heat treatment experiments. These particles were produced at 1900 °C. The EPMA images (Figures 5(d) to (f)) confirm the presence of Si in the  $\beta$ -SiC particles. The charcoal- and coal-converted  $\beta$ -SiC particles did not have any unreacted carbon in them, whereas some unreacted carbon was present in the petroleum coke-converted SiC (Figure 5(f)), indicating that the particle had not completely transformed to  $\beta$ -SiC even at 1900 °C. Figure 6 shows SEM morphologies of the  $\beta$ -SiC particles from charcoal (Figures 6(a), (d), and (g)), coal (Figures 6(b), (e), and (h)), and petroleum coke (Figures 6 (c), (f), and (i)), after they were heat-treated at 2100 °C, 2300 °C, and 2450 °C, respectively. The new crystals formed were dense and shaped as hexagonal-plates. More such crystals formed as the temperature increased.

The X-ray diffractograms of the samples were analyzed using Topas. As  $\beta$ -SiC was the main constituent in the preliminary material used for the experiments, it was included in the Rietveld refinement by Topas. Besides the already identified phases, *i.e.*, Si and SiC, most of the  $\beta$ -SiC samples produced from coal and petroleum coke showed a broad peak at around  $2\theta = 26$  deg. This could

**Table I. Raw Materials and Experimental Conditions Set for Conversion to  $\alpha$ -SiC**

Experiment No.	Raw Material	Quantity of Elemental Si in $\beta$ -SiC (Wt Pct)	Temperature ( $^{\circ}$ C) and Holding Duration
A1 to A3	charcoal-converted $\beta$ -SiC produced at 1750 $^{\circ}$ C	0	2100/2300/2450 1 h
A4 to A6	charcoal-converted $\beta$ -SiC produced at 1900 $^{\circ}$ C	9	2100/2300/2450 1 h
A7 to A9	charcoal-converted $\beta$ -SiC produced at 1900 $^{\circ}$ C	39	2100/2300/2450 1 h
B1 to B3	coal-converted $\beta$ -SiC produced at 1900 $^{\circ}$ C	9	2100/2300/2450 1 h
B4 to B6	coal-converted $\beta$ -SiC produced at 1900 $^{\circ}$ C	24	2100/2300/2450 1 h
C1 to C3	petroleum coke-converted $\beta$ -SiC produced at 1850 $^{\circ}$ C and 1900 $^{\circ}$ C	8.7	2100/2300/2450 1 h
C4 to C6	petroleum coke-converted $\beta$ -SiC produced at 1850 $^{\circ}$ C and 1900 $^{\circ}$ C	18.8	2100/2300/2450 1 h

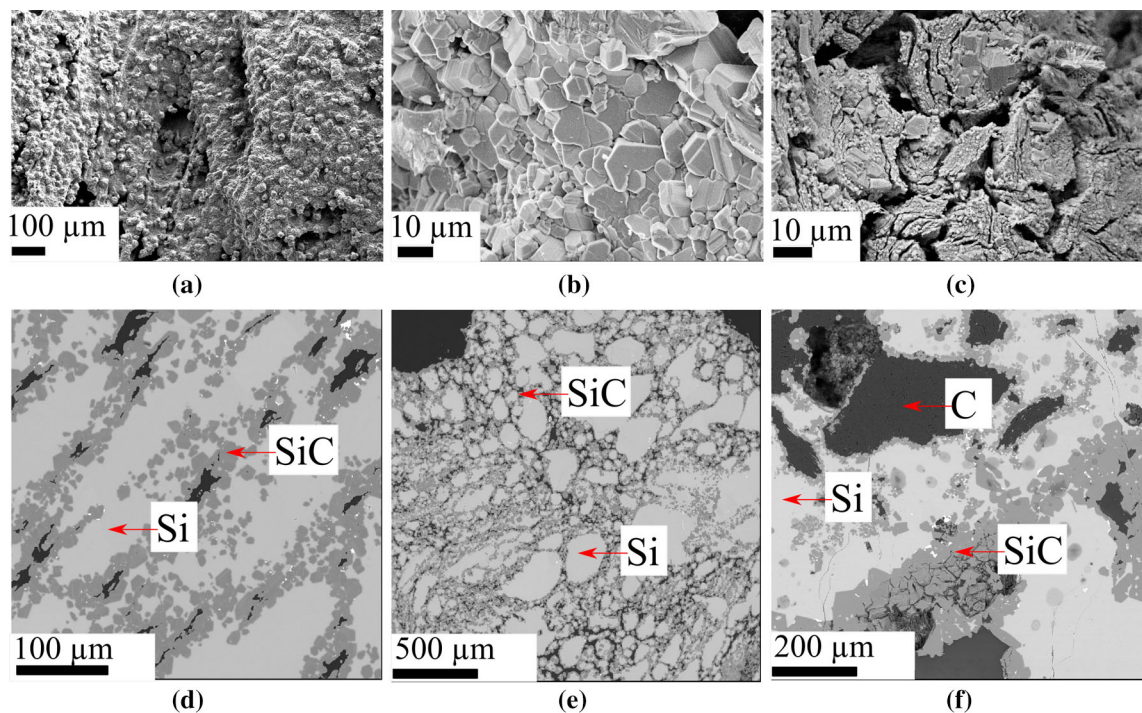


Fig. 5—SEM morphologies (top) and corresponding EPMA images (bottom) of  $\beta$ -SiC particles produced in the induction furnace at 1900  $^{\circ}$ C from charcoal ((a) and (d)), coal ((b) and (e)), and petroleum coke ((c) and (f)).

be arising from the unreacted carbon phase in the initial  $\beta$ -SiC particles and was not quantified in the analysis. The presence of the  $\alpha$ -SiC polytypes such as 4H, 6H, and 15R were established from their isolated peaks in the XRD data.

Figure 7 shows the X-ray diffractograms of charcoal-converted  $\beta$ -SiC particles with 9 wt pct Si and 39 wt pct Si in it. Prior to heating, these samples had higher intensities of Si. However, upon heating, intensities of the Si peaks decreased gradually. The samples exhibited a variety of structural polymorphs of SiC, in particular 3C and 6H. The SiC phases showed considerable

evidence of disorder/stacking faults, resulting in peak broadening in the 3C-SiC (111) position. The high intensity of stacking faults caused by defects in the SiC crystals has led to extra peaks at  $2\theta = 33.7$  deg and 38.3 deg. These high densities of defects in the starting material are also involved in the  $\beta$  to  $\alpha$  transformation; the heavily twinned  $\beta$ -SiC provides a high density of sites for the  $\alpha$ -SiC nucleation.<sup>[25]</sup> From Figure 7(b) it is evident that heating a SiC particle having high intensity Si peaks (39 wt pct Si) causes peak broadening and formation of new peaks at the 3C (111) position. The quantity of Si in the SiC enhanced the extent of  $\alpha$



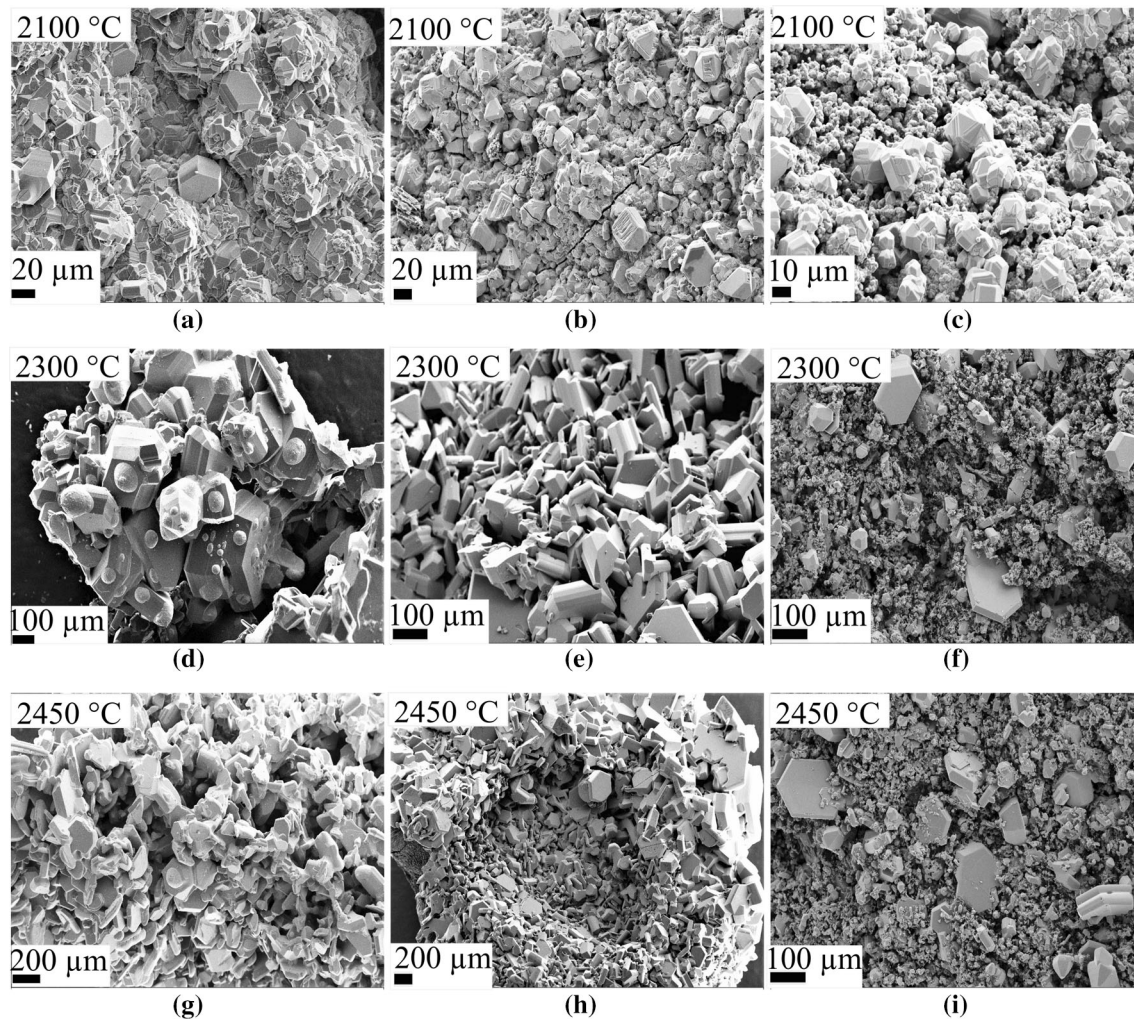


Fig. 6—SEM morphologies of  $\beta$ -SiC particles from charcoal ((a), (d), and (g)), coal ((b), (e), and (h)), and petroleum coke ((c), (f), and (i)) after heat treatment at 2100 (top), 2300 (middle), and 2450 °C (bottom).

transformation in this case. However, Figure 8 shows that in a SiC particle with hardly any amount of Si, the stacking fault reduced initially, and the peak broadening disappeared at 2100 °C. In this case, a higher temperature was required to transform  $\beta$ -SiC to  $\alpha$ -SiC.

Figure 9 shows SiC polytypes in the heat-treated, charcoal-converted  $\beta$ -SiC samples, quantitatively identified by Topas. The  $\beta$ -SiC without any Si in it did not transform to  $\alpha$ -SiC at 2100 °C. However, 64 wt pct of it converted to  $\alpha$ -SiC after the heat treatment at 2300 °C and showed the presence of main  $\alpha$ -SiC polymorphs such as 4H, 6H, and 15R in them.  $\beta$ -SiC particles with 9 wt pct elemental Si in them also did not transform to  $\alpha$ -SiC at 2100 °C. Nevertheless, heat-treating them at 2300 °C transformed 78 wt pct of the particles to  $\alpha$ -SiC. On the other hand,  $\beta$ -SiC with 39 wt pct Si transformed to 19 wt pct of  $\alpha$ -SiC at 2100 °C. This shows that  $\beta$ -SiC particles with 0 and 9 wt pct of Si require a temperature of about 2300 °C for the partial conversion to  $\alpha$ -SiC. At 2450 °C,  $\beta$ -SiC with 0, 9 and 39 wt pct of elemental Si transformed to 82, 91 and 100 wt pct of  $\alpha$ -SiC, respectively. There was hardly any 3C-SiC

phase detected in the  $\beta$ -SiC with 39 wt pct elemental Si after it was heat-treated at 2450 °C. However, around 4 wt pct of 3C phase was present after it was heat-treated at 2300 °C. This indicates that the stability of different phases is dependent on the amount of Si present in the SiC particles.

Figure 10 shows the X-ray diffractograms of coal-converted  $\beta$ -SiC samples with 9 and 24 wt pct Si, showing the SiC phases in them, both before and after they were heat-treated at 2100 °C, 2300 °C, and 2450 °C. More  $\alpha$ -SiC polytypes were detected in the  $\beta$ -SiC sample with 24 wt pct Si at 2300 °C (Figure 10(b)), indicating that the presence of Si in SiC had a major influence on  $\beta$ -SiC transforming to  $\alpha$ -SiC. Figure 11 shows the quantitative polytype analysis of the coal-converted  $\beta$ -SiC samples with varying amounts of Si, heated at 2100 °C, 2300 °C, and 2450 °C. At 2100 °C, the  $\beta$ -SiC samples containing 9 and 24 wt pct of pure Si, did not transform to  $\alpha$ -SiC. However, at 2300 °C,  $\beta$ -SiC sample with 9 wt pct Si partly transformed to  $\alpha$ -SiC, and 6H was the main polytype detected in it. The  $\beta$ -SiC sample with 24 wt pct Si transformed to

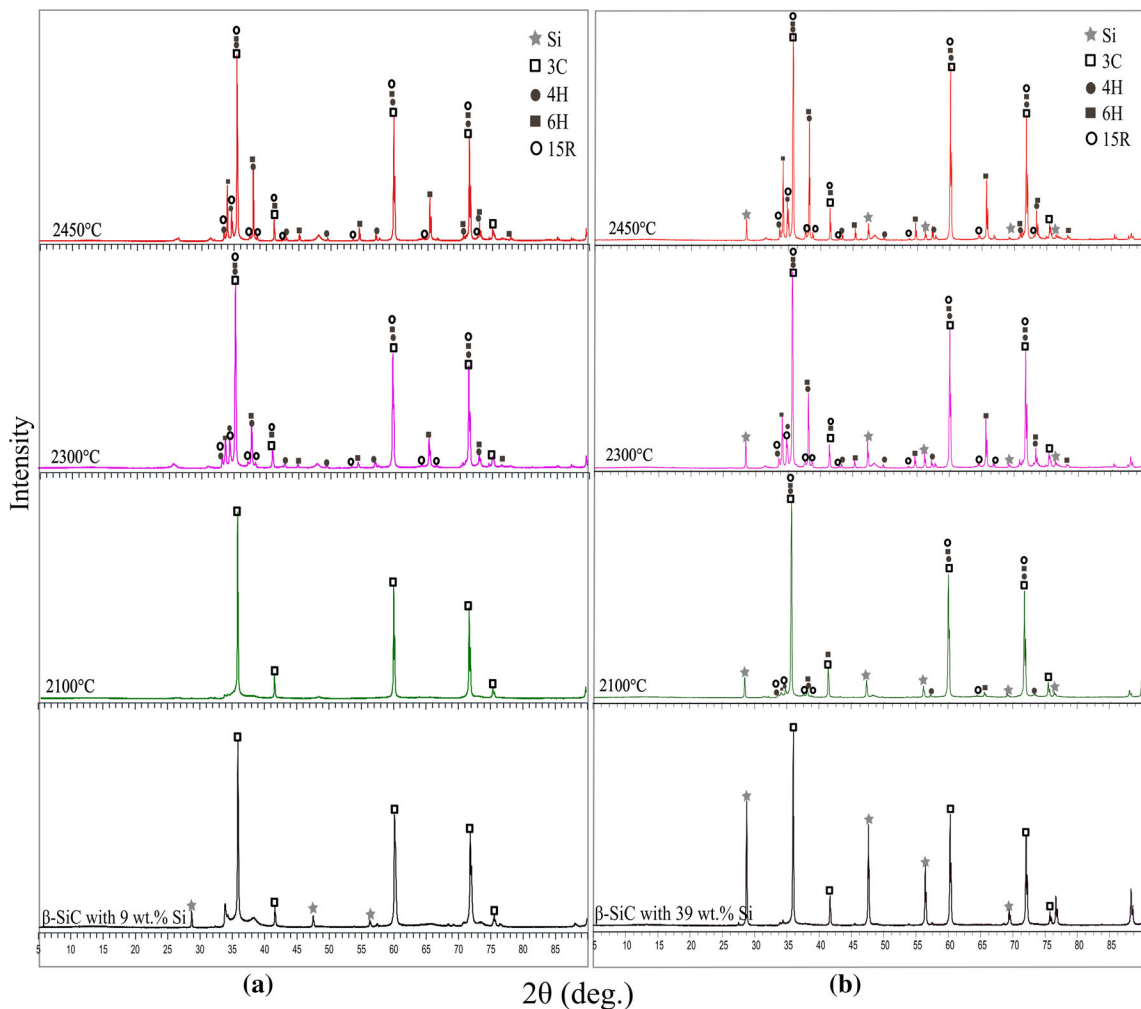


Fig. 7—X-ray diffractograms showing SiC phases identified in  $\beta$ -SiC (formed at 1900 °C from charcoal) with (a) 9 wt pct Si and (b) 39 wt pct Si, before and after the heat treatments at 2100 °C, 2300 °C, and 2450 °C.

43 wt pct of  $\alpha$ -SiC, at 2300 °C, and the polytypes 4H, 6H, and 15R were found in it. At 2450 °C,  $\beta$ -SiC samples with 9 and 24 wt pct Si transformed to 50 and 86.6 wt pct of  $\alpha$ -SiC, respectively.

Figure 12 shows the X-ray diffractograms of petroleum coke-converted  $\beta$ -SiC samples with 8.7 and 18.8 wt pct Si, which were heat-treated at 2100 °C, 2300 °C, and 2450 °C. Figure 13 shows the quantitative polytype analysis of the  $\beta$ -SiC samples with 8.7 and 18.8 wt pct elemental Si, heated at 2100 °C, 2300 °C, and 2450 °C. No  $\alpha$ -SiC had formed at 2100 °C and at 2300 °C, samples had partly converted to  $\alpha$ -SiC and only 6H phase was present. At 2450 °C,  $\beta$ -SiC samples with 18.8 wt pct Si had 6H as the dominating polytype and a minor percentage of 15R was also present in them. However,  $\beta$ -SiC samples with 8.7 wt pct of elemental Si, heated at 2450 °C, did not show any polytypes other than 3C and 6H. The major SiC polytype in  $\beta$ -SiC with 8.7 wt pct Si was 22 wt pct of 3C. The rest had transformed to 6H. The main SiC polytypes of 3C (24 wt pct), 6H (71 wt pct), and 15R (5 wt pct) had formed in  $\beta$ -SiC with 18.8 wt pct Si.

Samples of SiC from three industrial Si furnaces in Norway were procured to validate the laboratory production of  $\alpha$ -SiC. The first sample, SiC-ELT, was obtained from a built-up of SiC heap in the center of a furnace at Elkem Thamshavn. The second sample SiC-ELB was obtained from the furnace excavated at Elkem Bremanger and the third sample SiC-ELK was obtained from the center portion of one of the furnaces at Elkem Kristiansand. Coal was the main carbon source in all these furnaces. SiC polytypes in the three industrial SiC samples were quantitatively summarized from their XRD data and is shown in Figure 14. All samples consisted of the major SiC polytypes such as 3C, 4H, 6H, and 15R, with 6H being the main polytype. The amount of  $\alpha$ -SiC was calculated as 78, 87, and 95 wt pct in SiC-ELB, SiC-ELT, and SiC-ELK, respectively. Hardly any cubic form of SiC, *i.e.*, 3C, was present in the SiC-ELK sample and it had completely transformed to  $\alpha$ -SiC crystal. The major phase in it was 86 wt pct of 6H, followed by ~ 3 wt pct of 4H and ~ 6 wt pct of 15R. Elemental Si of around 1 to 4 wt pct was found in all the samples.

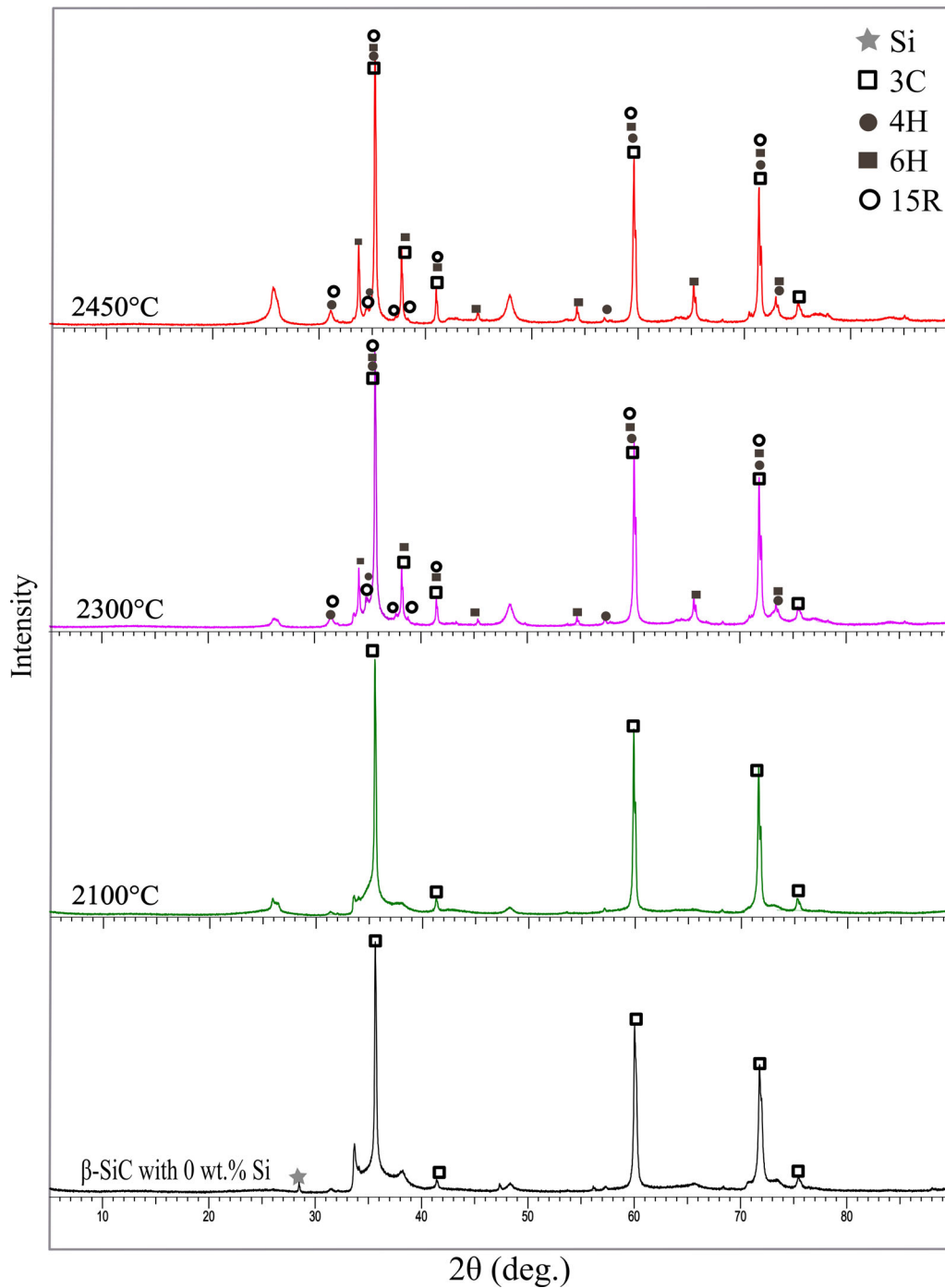


Fig. 8—X-ray diffractograms showing SiC phases identified in  $\beta$ -SiC formed at 1750 °C from charcoal with 0 wt pct Si, before and after heat treatments at 2100 °C, 2300 °C, and 2450 °C.

#### IV. DISCUSSION

The analyses showed that transformation of  $\beta$ -SiC to  $\alpha$ -SiC occurs at temperatures  $\geq 2100$  °C.  $\beta$ -SiC with 0 wt pct Si did not transform to  $\alpha$ -SiC until 2100 °C. However, increasing the temperature to 2300 °C enhanced the formation of  $\alpha$ -SiC in it. Figure 15 shows the charcoal-converted  $\beta$ -SiC with no elemental Si in it, heat-treated at 2100 °C to 2450 °C. It shows that temperature is one of the main factors determining the

transformation to  $\alpha$ -SiC. This is in accordance with previous literature stating that temperature is a main factor influencing the polytype transformation in SiC.<sup>[12,21]</sup> An increase in temperature leads to a higher thermal diffusion of atoms in the cubic form of  $\beta$ -SiC (3C). A rearrangement of atoms within the SiC would thus lead to the formation of different  $\alpha$ -SiC polytypes (Figure 1(a)).<sup>[20,21]</sup>



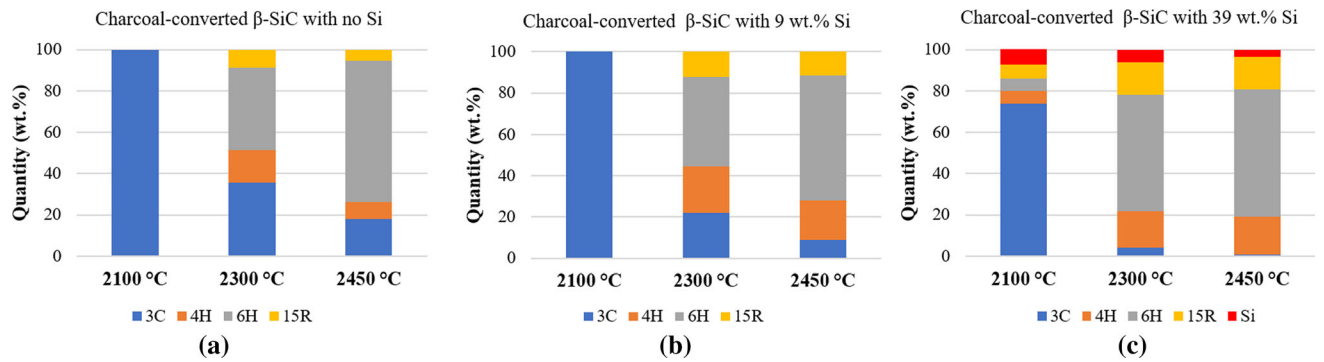


Fig. 9—Summary of quantitative SiC polytypes formed in  $\beta$ -SiC with (a) no additional amount of Si, (b) 9 wt pct Si, and (c) 39 wt pct Si, after they were heat-treated at 2100 °C, 2300 °C, and 2450 °C.

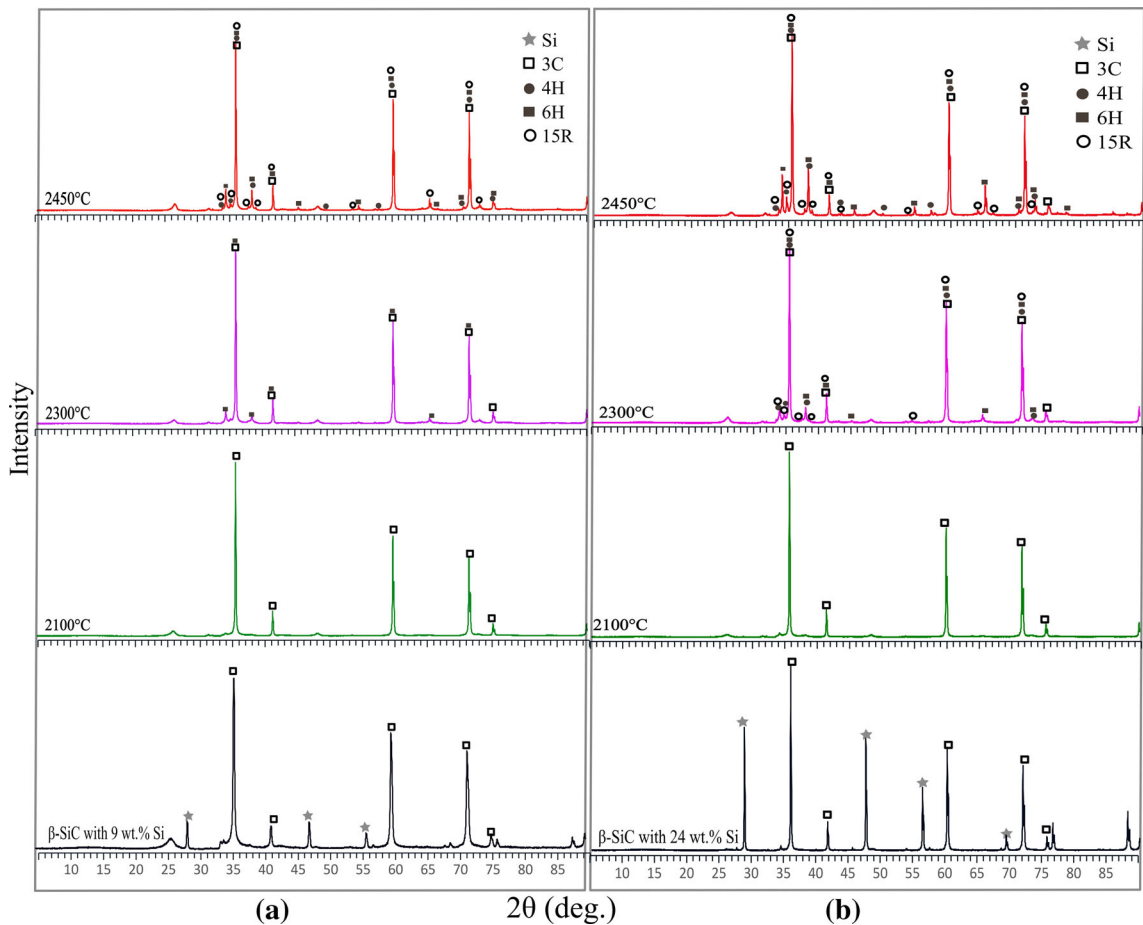


Fig. 10—X-ray diffractograms identifying the SiC phases in  $\beta$ -SiC with (a) 9 wt pct Si and (b) 24 wt pct Si, produced from coal at 1900 °C, and heat-treated at 2100 °C, 2300 °C, and 2450 °C.

The results also revealed that the presence of elemental Si in the SiC particles enhanced the extent of transformation of  $\beta$ -SiC to  $\alpha$ -SiC. Figure 16 shows the charcoal-converted  $\beta$ -SiC with 0, 9, and 39 wt pct of elemental Si heat-treated at 2100 °C to 2450 °C. The evolution of  $\alpha$ -SiC in the samples clearly shows that along with temperature, the amount of Si in the SiC particles has also caused an increase in their

hexagonality. Approximately 20 wt pct of the  $\beta$ -SiC with 39 wt pct Si in it transformed to  $\alpha$ -SiC even at 2100 °C. Ringdalen<sup>[19]</sup> heat-treated  $\beta$ -SiC derived from coal (0 wt pct Si) at 2000 °C to 2500 °C and found that no transformation to  $\alpha$ -SiC occurred until 2200 °C. The present study revealed that elemental Si in the  $\beta$ -SiC particles could bring forth transformation to  $\alpha$ -SiC even at 2100 °C.

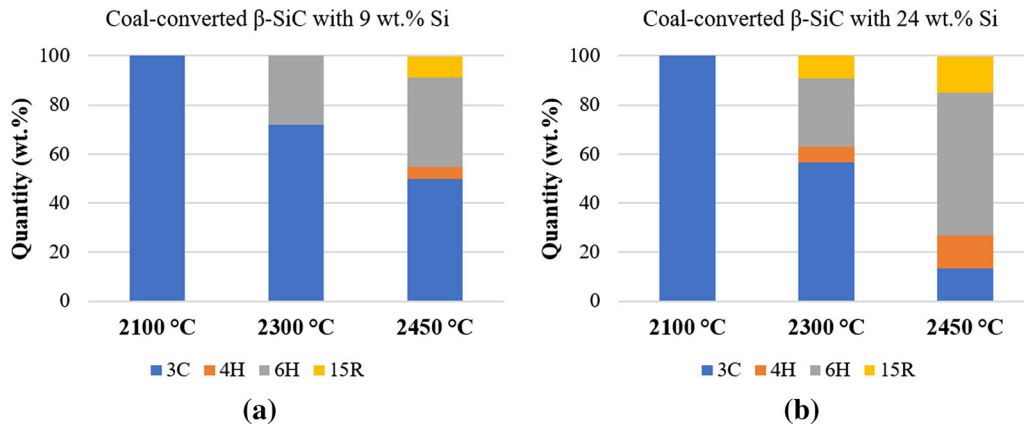


Fig. 11—Quantitative polytype analysis of coal-converted  $\beta$ -SiC samples with (a) 9 and (b) 24 wt pct of Si, heat-treated at 2100 °C, 2300 °C, and 2450 °C.

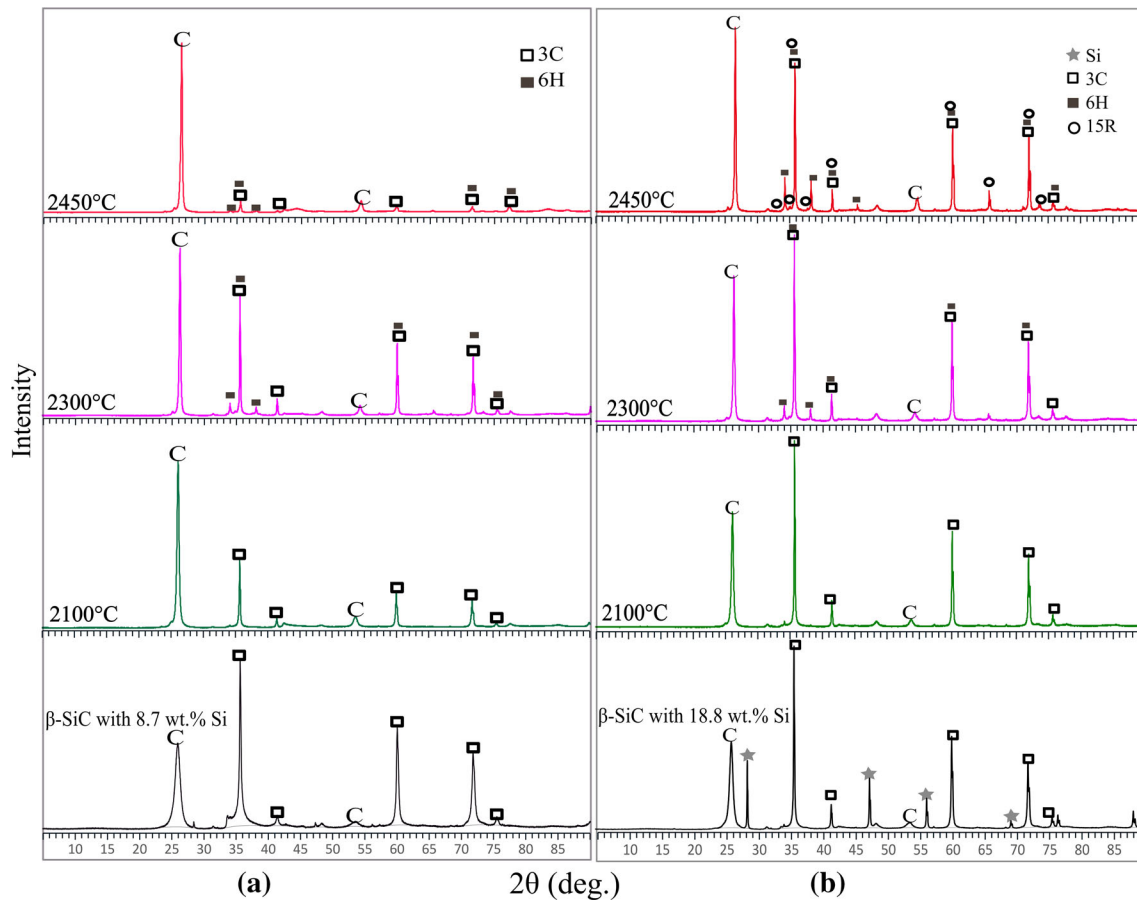


Fig. 12—X-ray diffractograms of identified SiC phases in the  $\beta$ -SiC with (a) 8.7 wt pct Si and (b) 18.8 wt pct Si formed at 1850 °C and 1900 °C from petroleum coke, and after it is heat-treated at 2100 °C, 2300 °C, and 2450 °C.

The properties of original carbon source also determine the extent of transformation to  $\alpha$ -SiC. Figure 17 summarizes the effect of temperature, type of the carbon material, and Si content in  $\beta$ -SiC on the transformation to  $\alpha$ -SiC. It shows that both elemental Si and the original carbon source are essential factors determining the extent of  $\alpha$ -SiC conversion. Charcoal-converted

$\beta$ -SiC with elemental Si had the highest extent of transformation to  $\alpha$ -SiC, compared with coal and petroleum coke. The physical properties of the carbon materials such as their porosities and surface areas are presented in Table II. Charcoal has the highest porosity and the largest surface area compared with coal and petroleum coke. Larger surface area indicates a higher

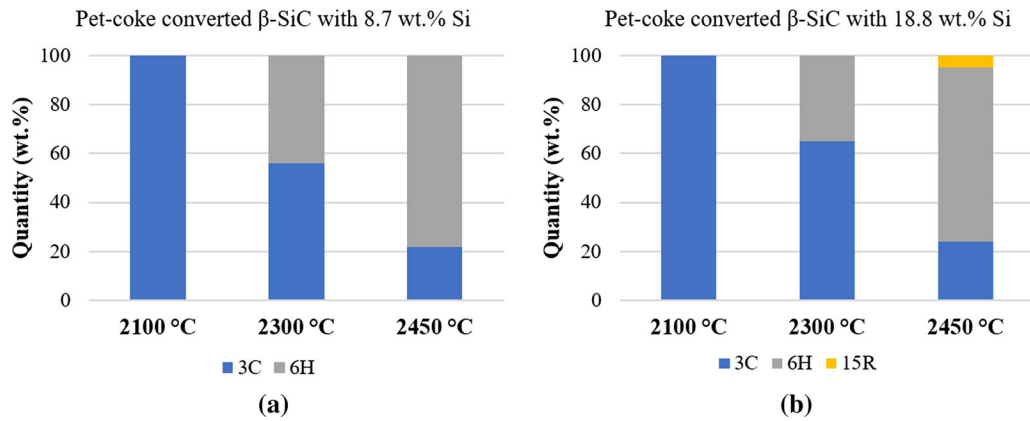


Fig. 13—Quantitative polytype analysis of petroleum coke-converted  $\beta$ -SiC samples with (a) 8.7 and (b) 18.8 wt pct elemental Si, heat-treated at 2100 °C, 2300 °C, and 2450 °C.

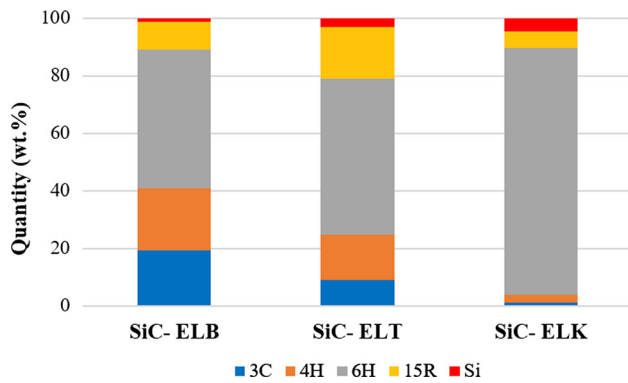


Fig. 14—SiC polytypes present in the three industrial SiC samples formed during Si process.

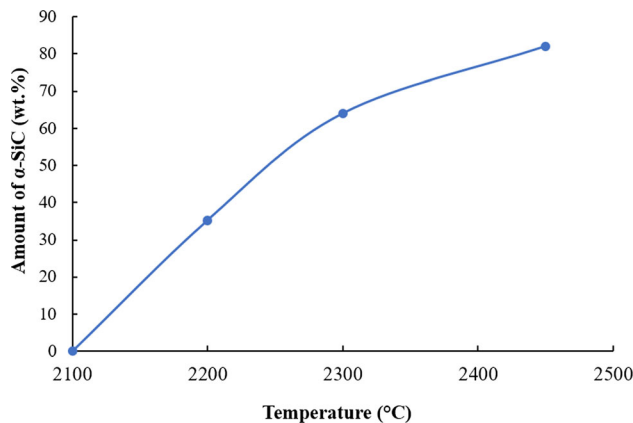


Fig. 15—Charcoal-converted  $\beta$ -SiC with no elemental Si in it, heat-treated at 2100 °C to 2450 °C.

availability of nucleation sites for the  $\alpha$ -SiC phases. The thermodynamic driving force for both nucleation and crystal growth increase with surface area,<sup>[26]</sup> which could be the main reason for the higher extent of transformation in the charcoal-converted  $\beta$ -SiC.

The extent of  $\alpha$ -SiC formation was higher in the industrial SiC samples than the laboratory-produced samples. Previous studies have shown that impurities such as nitrogen (N), aluminum (Al), boron (B), Calcium (Ca), and oxygen (O) act as a catalyst for the transformation of  $\beta$ -SiC to  $\alpha$ -SiC.<sup>[10,12,27]</sup> However, results from the EPMA elemental mapping and XRD analysis did not show presence of any of these impurities in the  $\beta$ -SiC particles produced from charcoal, coal, and petroleum coke in this study. Figure 18 represents the elemental distribution in charcoal-converted  $\beta$ -SiC samples produced at 1900 °C. Hardly any impurity was present, and the particle mainly consisted of Si and SiC. Traces of iron (Fe) were also observed in the samples. Therefore, it is presumed that in the present study, impurities in the chosen carbon materials did not play any significant role in the transformation to  $\alpha$ -SiC.

Figure 19 shows the elemental mapping of one of the industrial SiC samples. All industrial samples had similar elemental distribution and showed presence of Fe, Al, Ca, and O in them. Therefore, it could be inferred that during the industrial Si production, along with temperature and high amounts of elemental Si in the SiC, impurities might also have enhanced the extent of transformation to  $\alpha$ -SiC. The laboratory-produced SiC samples were only exposed to a CO(g) atmosphere, whereas the gas atmosphere in an industrial furnace is a combination of a higher partial pressures of SiO(g) along with CO(g). In addition, the industrial samples might have been exposed to higher temperatures over days and weeks, not just hours. All these factors could have influenced the extent of  $\alpha$ -SiC formation in the industrial SiC samples.

The distribution of polytypes in the  $\alpha$ -SiC varied between the samples produced from various carbon sources. Figures 20 and 21 show the polytype distribution in  $\alpha$ -SiC samples produced from  $\beta$ -SiC with ~ 9 wt pct Si in it, respectively at 2300 °C and 2450 °C. Both charcoal- and coal-converted  $\beta$ -SiC with 9 wt pct Si showed formation of 4H, 6H, and 15R at 2450 °C. In  $\beta$ -SiC with 8.7 wt pct Si from petroleum coke, only the 6H polytype was present at 2300 °C and 2450 °C. Even though coal with 9 wt pct Si had the least amount of



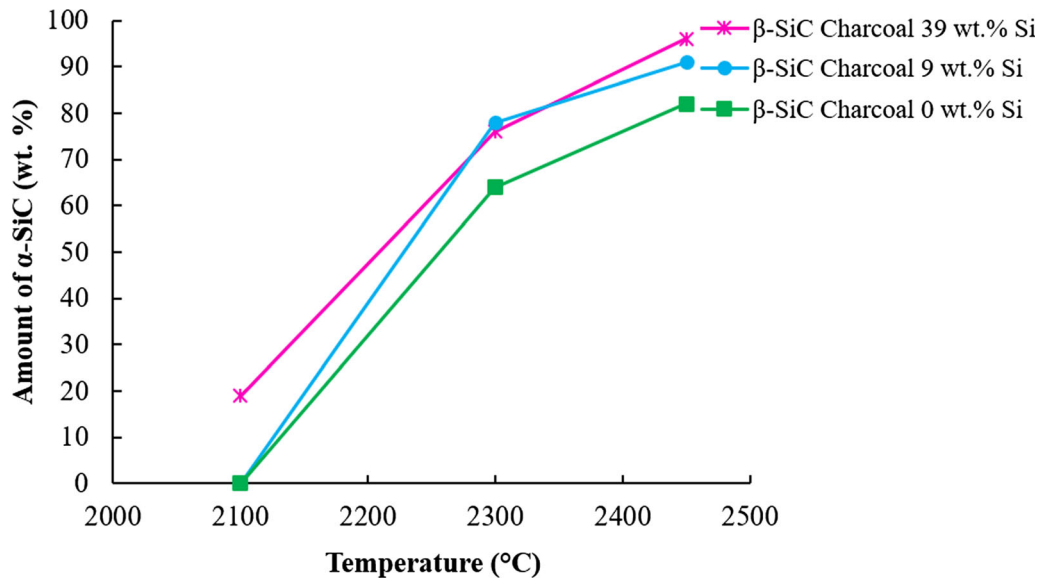


Fig. 16—Charcoal-converted  $\beta$ -SiC with 0, 9, and 39 wt pct of elemental Si, heat-treated at 2100 °C to 2450 °C.

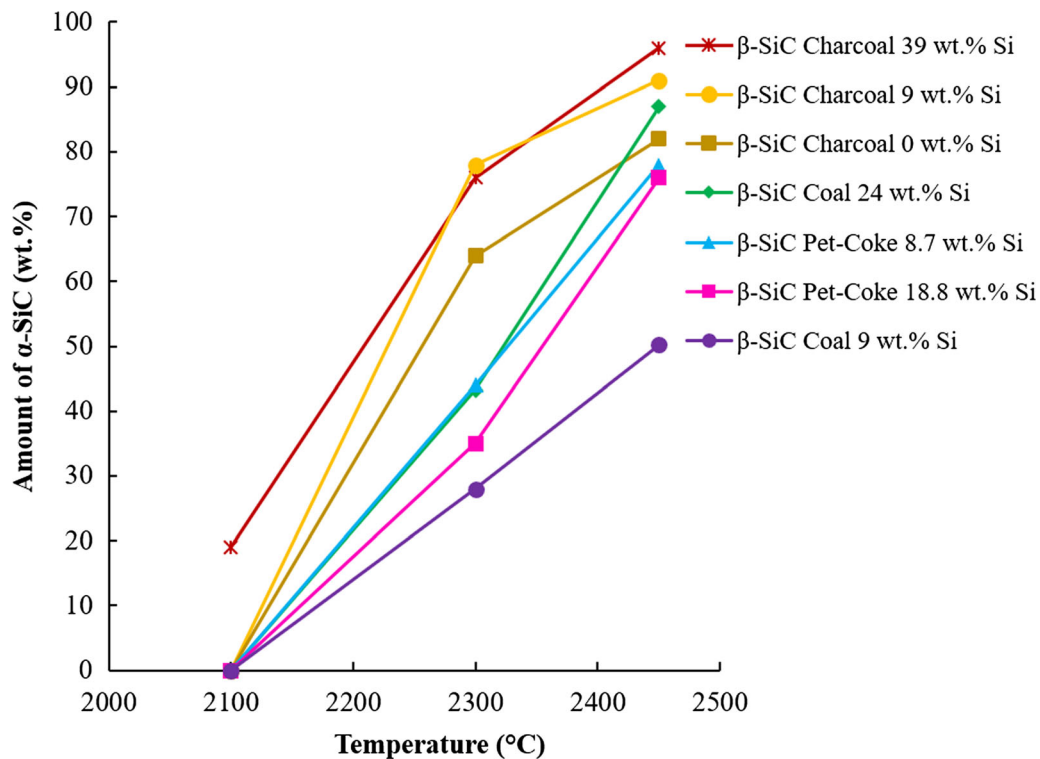


Fig. 17—Effect of temperature, type of the original carbon material, and Si content in  $\beta$ -SiC, on transformation to  $\alpha$ -SiC.

**Table II. Porosities and Surface Areas of Charcoal, Coal, and Petroleum Coke**

Carbon Material	Porosity (Pct)	Surface Area ( $\text{m}^2/\text{g}$ )
Charcoal	75	98.41
Coal	56	1.25
Petroleum coke	20	0.30

$\alpha$ -SiC in it (purple line in Figure 17), more polytypes of  $\alpha$ -SiC developed in it at 2450 °C, compared with petroleum coke (Figure 21).

Thermodynamically, SiC could also form as several gas species at temperatures higher than 2000 °C. Figure 22 shows the equilibrium partial pressures of SiC gas species at temperature > 2000 °C, calculated using the HSC Chemistry 9 software. If elemental Si and  $\beta$ -SiC samples are exposed to a temperature near or above the

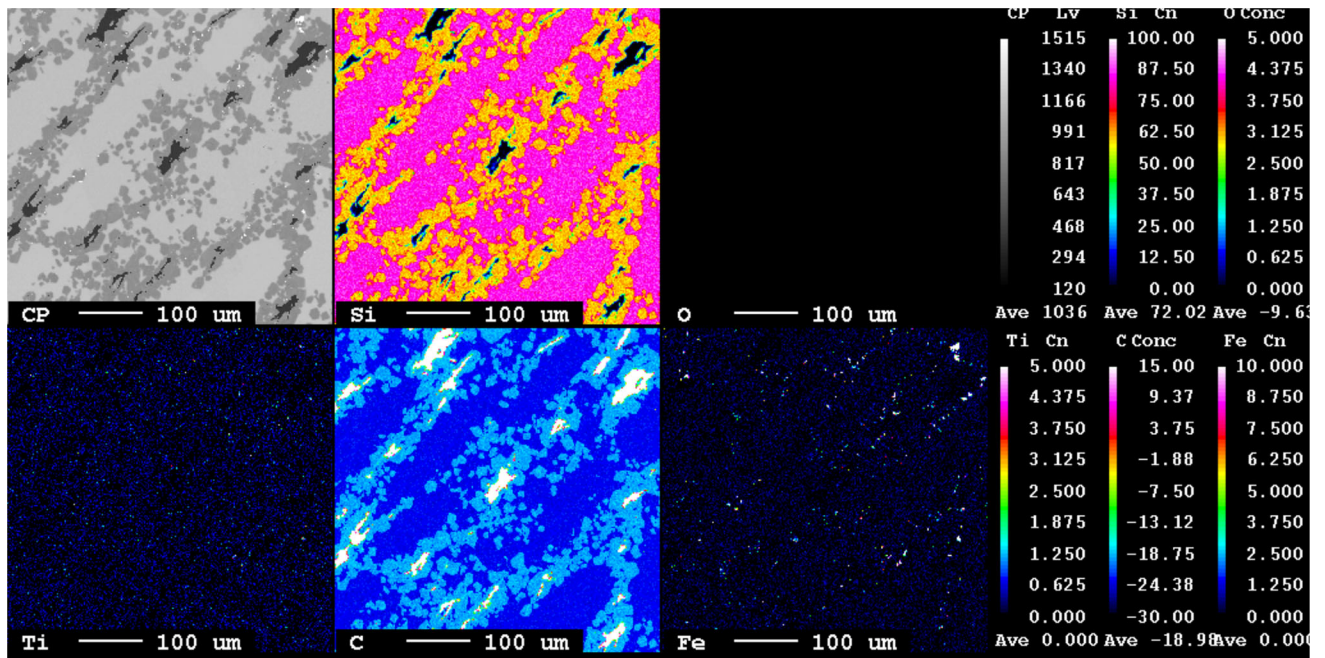


Fig. 18—Elemental mapping of charcoal-converted  $\beta$ -SiC particle produced at 1900 °C.

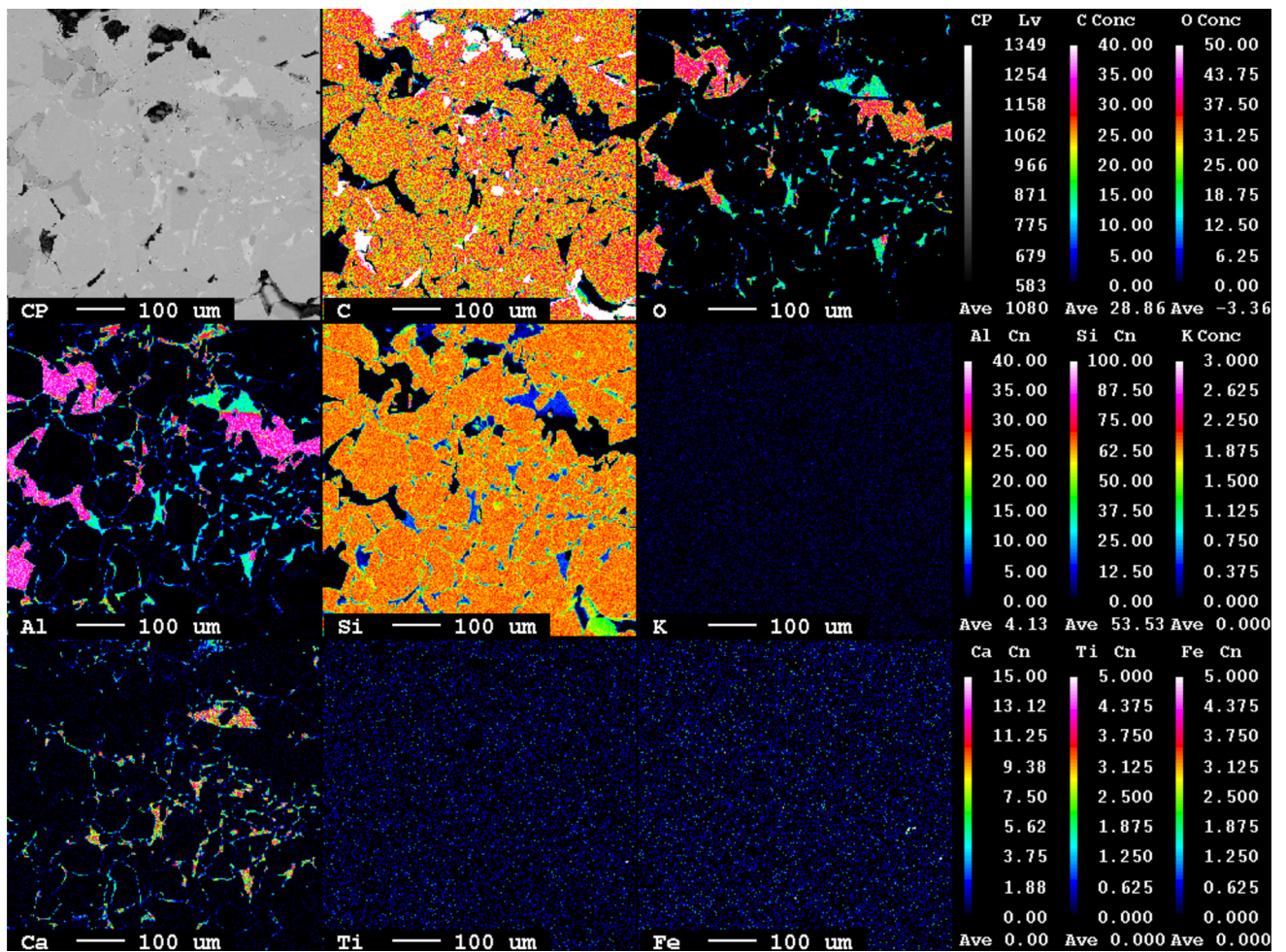


Fig. 19—EPMA of and elemental distribution in an industrial SiC sample.



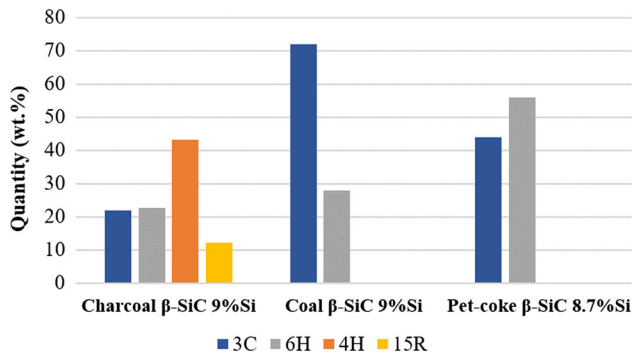


Fig. 20—SiC polytype distribution in  $\alpha$ -SiC formed at 2300 °C from charcoal, coal, and petroleum coke.

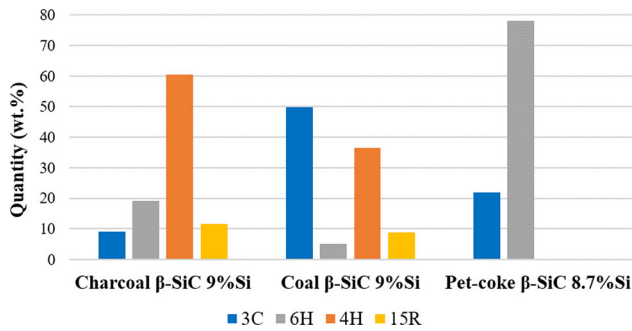


Fig. 21—SiC polytype distribution in  $\alpha$ -SiC formed at 2450 °C from charcoal, coal, and petroleum coke.

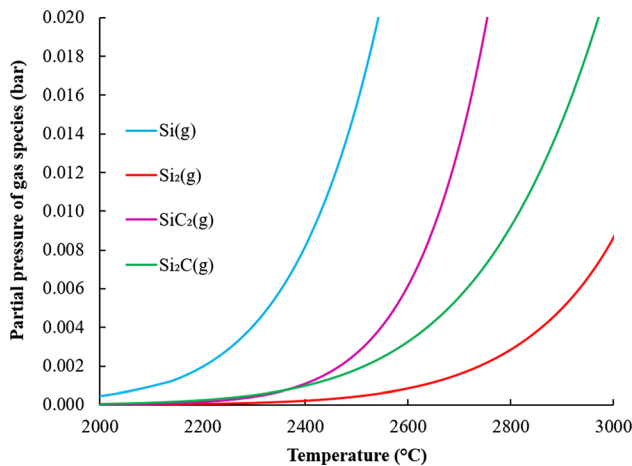


Fig. 22—Equilibrium partial pressures of SiC gas species at 2000 °C to 3000 °C.

decomposition temperature of SiC, gas species rich in Si and carbon such as Si(g) and SiC<sub>2</sub>(g) would form at a higher partial pressure. The partial pressures of Si(g) and SiC<sub>2</sub>(g) are higher than those of the other gas species of Si and carbon formed at these temperatures. Kong *et al.*<sup>[28]</sup> performed a detailed study regarding the possible reactions responsible for the formation of SiC from the gas species. Based on the equilibrium

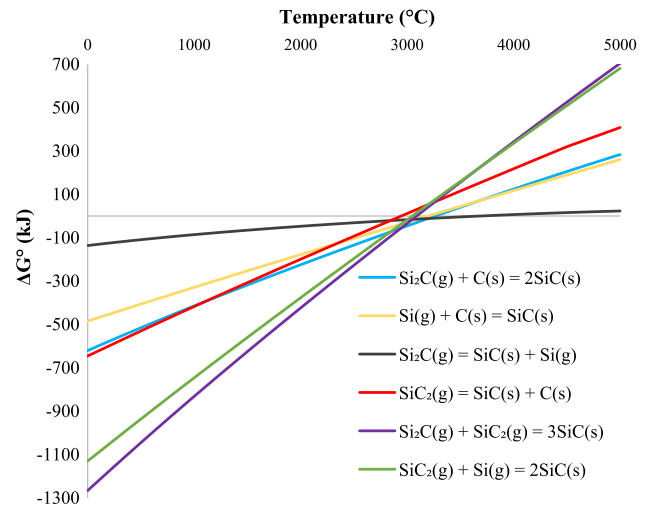
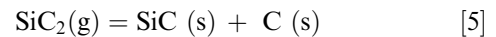


Fig. 23—Free energy values of the possible reactions responsible for the formation of SiC from gas species.

concentration of the gas species and the free energy values of reactions, it is probable that the SiC could form from the gas species by the reactions between Si(g) and SiC<sub>2</sub>(g) as follows:



Between these two reactions, Reaction [6] has the largest negative free energy, making it more stable than Reaction [5]. Figure 23 shows the evolution of free energy values of the possible reactions responsible for the formation of SiC from the gas species corresponding to an increasing temperature, calculated using the HSC Chemistry 9 software. The higher gas pressures of Si and SiC<sub>2</sub> species might facilitate the reaction between these two gas species to form  $\alpha$ -SiC, in accordance to Reaction [6]. Some of these gas species might precipitate as  $\alpha$ -SiC at high temperatures, forming dendritic structures as found in the industrial  $\alpha$ -SiC samples.<sup>[16]</sup>

## V. CONCLUSIONS

Various excavation reports have revealed that as  $\beta$ -SiC formed in the outer zone comes to the inner zone of the furnace, the higher temperatures transform it to  $\alpha$ -SiC containing various polymorphs of SiC. To study the structural variations occurring in SiC at these higher temperature zones, heat treatment experiments were performed in the graphite tube furnace at temperature ranges of 2100 °C to 2450 °C. The predominantly used carbon sources in the Si production process such as charcoal, coal, and petroleum coke were used in this study. Two types of  $\beta$ -SiC, one without any elemental Si and other with varying amounts of elemental Si in them



were heat-treated. Results from the heat treatment experiments showed that there are three main factors that influence the extent of transformation to  $\alpha$ -SiC; the temperature, amount of elemental Si in the  $\beta$ -SiC particles, and type of the carbon material that produced the  $\beta$ -SiC. The charcoal-converted  $\beta$ -SiC particles easily transformed to  $\alpha$ -SiC at 2100 °C, compared with the  $\beta$ -SiC from coal and petroleum coke. Moreover, a higher amount of elemental Si in SiC particles enabled the formation of  $\alpha$ -SiC at 2100 °C.

In addition, SiC could also form as gas species at temperatures above 2000 °C. As these gases flow to regions of relatively lower temperatures in the furnace, they condense at around 2000 °C. Most of the gases condense into solid SiC ( $\alpha$ -SiC) and elemental Si. As Si(g) and SiC<sub>2</sub>(g) has higher equilibrium concentrations than the other carbon and Si bearing gas species, these two gases could react together to form precipitates of  $\alpha$ -SiC at temperatures lower than 2000 °C.

The quantities of  $\alpha$ -SiC polytypes in the industrial samples were higher compared with the  $\alpha$ -SiC samples produced in the laboratory. In the industrial Si process, along with higher temperatures and higher amounts of elemental Si in the SiC, impurities might also have enhanced the extent of transformation to  $\alpha$ -SiC. The laboratory SiC samples were exposed only to a CO(g) atmosphere, whereas the gas atmosphere in an industrial furnace is a combination of a higher partial pressures of SiO(g) along with CO(g). In addition, the industrial samples might have been exposed to higher temperatures over days and weeks, not just hours, which might have influenced the formation of  $\alpha$ -SiC in them.

#### ACKNOWLEDGMENTS

Metal Production, an eight-year research center under the SFI-scheme (Centers for Research-based Innovation, 237738) has funded this work. The authors gratefully acknowledge the financial support from the Research Council of Norway and the partners of SFI Metal Production.

#### FUNDING

Open Access funding provided by NTNU Norwegian University of Science and Technology (incl St. Olavs Hospital - Trondheim University Hospital).

#### OPEN ACCESS

This article is licensed under a Creative Commons Attribution 4.0 International License, which permits use, sharing, adaptation, distribution and reproduction in any medium or format, as long as you give appropriate credit to the original author(s) and the source, provide a link to the Creative Commons licence, and indicate if changes were made. The images or other

third party material in this article are included in the article's Creative Commons licence, unless indicated otherwise in a credit line to the material. If material is not included in the article's Creative Commons licence and your intended use is not permitted by statutory regulation or exceeds the permitted use, you will need to obtain permission directly from the copyright holder. To view a copy of this licence, visit <http://creativecommons.org/licenses/by/4.0/>.

#### REFERENCES

1. G.L. Harris: *Properties of Silicon Carbide*, INSPEC, the institution of Electrical Engineers, United Kingdom, 1995.
2. H. Abderrazak and E.S.B.H. Hmida: Silicon Carbide: Synthesis and Properties, in *Properties and Applications of Silicon Carbide*, R. Gerhardt, ed., InTech, London, 2011, pp. 361–88.
3. L.H. Lindstad: *Recrystallization of Silicon Carbide*, Dr.ing. thesis, Department of Metallurgy, Norwegian University of Science and Technology, 2002.
4. A. Schei, J.K. Tuset, and H. Tveit: *Production of High Silicon Alloys*, Tapir, Trondheim, 1998.
5. V. Myrvågnes: *Analyses and characterization of fossil carbonaceous materials for silicon production*, Ph.D thesis, Institutt for materialteknologi, Norwegian University of Science and Technology, 2008.
6. E.H. Myrhaug: *Non-fossil reduction materials in the silicon process - properties and behaviour*, Dr.ing. thesis, Norwegian University of Science and Technology, 2003.
7. R.W. Olesinski and G.J. Abbaschian: *Bull. Alloy Phase Diagrams*, 1984, vol. 5 (5), pp. 486–89.
8. R.I. Scace and G.A. Slack: *J. Chem. Phys.*, 1959, vol. 30 (6), pp. 1551–55.
9. A.L. Ortiz, F. Sánchez-Bajo, F.L. Cumbreira, and F. Guiberteau: *J. Appl. Crystallogr.*, 2013, vol. 46 (1), pp. 242–47.
10. N.W. Jepps and T.F. Page: *Prog. Cryst. Growth Charact.*, 1983, vol. 7 (1-4), pp. 259–307.
11. D. Pandey and P. Krishna: *Prog. Cryst. Growth Charact.*, 1983, vol. 7 (1-4), pp. 213–58.
12. G.C. Trigunayat: *Solid State Ionics*, 1991, vol. 48 (1–2), pp. 3–70.
13. J.B. Casady and R.W. Johnson: *Solid-State Electron.*, 1996, vol. 39 (10), pp. 1409–22.
14. R. Han, X. Xu, X. Hu, N. Yu, J. Wang, Y. Tian, and W. Huang: *Opt. Mater.*, 2003, vol. 23 (1–2), pp. 415–20.
15. T. Lindstad, S. Gaal, S. Hansen, and S. Prytz: *Improved SINTEF SiO-Reactivity Test*, INFACON XI, New Dehli, 2007.
16. M. Tangstad, M. Ksiazek, and J.E. Andersen: *Zones and Materials in the Si Furnace*, Silicon for the Chemical and Solar Industry XII, Trondheim, 2014.
17. M. Ksiazek, M. Tangstad, and E. Ringdalen: *Five Furnaces Five Different Stories*, Silicon for the Chemical and Solar Industry XIII, Kristiansand, 2016.
18. G. Tranell, M. Andersson, E. Ringdalen, O. Ostrovski, and J.J. Steinmo: *Reaction Zones in a FeSi75 Furnace - Results from an Industrial Excavation*, The Twelfth International Ferroalloys Congress: Sustainable Future, Helsinki, 2010.
19. E. Ringdalen: *SiC Structures and SiC Transformations in Industrial Si-Production*, Silicon for the Chemical and Solar Industry XIV, Svølvar, 2018.
20. W.F. Knippenberg: *Philips Res. Rep.*, 1963, vol. 18, pp. 161–74.
21. W.S. Yoo and H. Matsunami: *Jpn. J. Appl. Phys.*, 1991, vol. 30 (3R), pp. 545–53.
22. S. Jayakumari and M. Tangstad: *Formation of Elemental Silicon in  $\beta$ -SiC Particles*, Silicon for the Chemical and Solar Industry XIV, Svølvar, 2018.
23. S. Jayakumari and M. Tangstad: *Silicon Carbide formation from Coal or Charcoal in the Silicon/Ferrosilicon Process*, Infacon XV: International Ferro-Alloys Congress, Cape Town, 2018.
24. C. Sindland: *Reactivity of Si and SiO<sub>2</sub> mixtures*, Specialisation Project, Norwegian University of Science and Technology, unpublished research, 2019.

25. A.L. Ortiz, F. Sánchez-Bajo, F.L. Cumbreira, and F. Guiberteau: *Mater. Lett.*, 2001, vol. 49 (2), pp. 137–45.
26. S. Stølen and T. Grande: *Chemical Thermodynamics of Materials: Macroscopic and Microscopic Aspects*, Wiley, Chichester, 2003.
27. P.A. Kistler-De Coppi and W. Richarz: *Int. J. High Technol. Ceram.*, 1986, vol. 2 (2), pp. 99–113.
28. P. Kong, R.M. Young, T.T. Huang, E. Pfender: *Beta-SiC synthesis in an atmospheric pressure convection-stabilized arc*, 7th Int Symp Plasma Chem, Eindhoven, The Netherlands, 1985, pp. 674.

**Publisher's Note** Springer Nature remains neutral with regard to jurisdictional claims in published maps and institutional affiliations.